JOURNAL OF PROPULSION AND POWER
Vol. 19, No. 5, September–October 2003

Magnetohydrodynamic Power Generation Experiments with Fuji-1 Blowdown Facility

Y. Okuno,* T. Okamura,* T. Suekane,† H. Yamasaki,* S. Kabashima,‡ and S. Shioda§
Tokyo Institute of Technology, Yokohama 226-8502, Japan

Experimental results of nonequilibrium plasma magnetohydrodynamic (MHD) power generation from the Fuji-1 blowdown facility are presented. The Fuji-1 experiments have been conducted since 1983, and the disk-shaped MHD generators called Disk-F3a, F3r, and F4 have been tested during the last decade. In the experiment with the newest Disk-F4 generator, which was designed based on the results of previous experiments with the Disk-F3a and F3r generators, an output power of 506 kW and an enthalpy extraction ratio of 18.4% for thermal input of 2.75 MW were simultaneously obtained. During the experiment, however, the deposition of seed material on the electrodes and the insulator walls was revealed, and large amount of impurity (water vapor) contamination in the working gas was detected. In the last experiment the stainless-steel-coated anodes were used instead of copper anodes to prevent the seed material from depositing on the generator walls, and the impurity contamination was reduced by increasing the bottom temperature of the heat exchanger. Consequently, an output power of 544 kW for thermal input of 3.38 MW and an enthalpy extraction ratio of 18.9% for thermal input of 2.17 MW were successfully demonstrated. Each value is the highest among those achieved with the Fuji-1 facility.

Introduction

IN the last few decades open- and closed-cycle magnetohydrodynamic (MHD) systems have been investigated and are continuing to be investigated as possible candidates for high-efficiency electrical power-generation applications.[1–4] In the open-cycle MHD power generation combustion gas is used as a working gas, where the plasma is in a thermal equilibrium state. In the closed-cycle MHD system, on the other hand, a nonequilibrium plasma, alkali metal seeded noble gas, is utilized as a working medium. One of the advantages of the closed-cycle MHD is that higher power density can be achieved because of the higher electrical conductivity in the generator channel. This fact leads to a compact generator with a smaller superconducting magnet as compared to the open-cycle MHD generator, although the closed-cycle power plant system is relatively complicated. Another advantage is that the high power generation is possible even under relatively low gas temperature, about 2000 K, because the electrical conductivity in the nonequilibrium plasma depends on the electron temperature and not on the gas temperature. Of course, higher gas temperature will also provide higher plant efficiency in a conventional thermodynamical system.

Studies on the closed-cycle MHD power generation have been conducted with the Fuji-1 blowdown facility at Tokyo Institute of Technology since 1983 (Ref. 5). One of the main objectives in the Fuji-1 experiments is to demonstrate the high enthalpy extraction ratio (electrical output/thermal input) with a disk-shaped generator for a period of several tens of seconds under low seed fractions. For this purpose attention has been paid to the achievement of stable and uniform nonequilibrium plasma with full seed ionization[6,7] under the condition of strong MHD interaction. In a disk MHD generator the electromotive force is induced by the radial plasma flow and the magnetic field applied perpendicularly to the flow and yields the azimuthal current (Faraday current). The interaction between the Faraday current and the magnetic field results in the radial Hall electric field. Thus, the electric power is extracted with a load resistance connected between inner (anode) and outer (cathode) electrodes. In the Fuji-1 blowdown facility the disk-shaped MHD generators called Disk-F3a, F3r, and F4 have been tested during the last decade, and the newest Disk-F4 generator has been in service since 1994 (Refs. 8–12).

The test results from the Disk-F3a and F3r generators[8,9] are reviewed briefly in this paper in order to clarify the aim and meaning of the experiment with the Disk-F4 generator. As will be described later, although the high performance has been demonstrated in the experiments with the Disk-F3a and F3r generators there was still room for improvement in the generator performance. The newest Disk-F4 generator was designed on the basis of the information obtained by scrutinizing the results of experiments with the Disk-F3a and F3r generators. Thus, the design concept of the Disk-F4 generator is mainly based on the reliability for high power generation. For this purpose, as will be mentioned in detail, the Mach number at the generator inlet is increased slightly as compared to those in the earlier generator designs. Furthermore, attention has been paid to the realization of suitable working gas conditions for high power generation.

In the experiment with the Disk-F4 generator, an output power of 506 kW and an enthalpy extraction ratio of 18.4% for thermal input of 2.75 MW were simultaneously obtained. In the experiments, however, the reduction of output power was observed at the early stage of the power-generation run, which could be attributed to the deposition of seed material on the water-cooled electrodes and insulator walls. Furthermore, a large amount of water vapor was detected in the working gas. In the last power-generation experiments with the Disk-F4 generator, the stainless-steel-coated anodes were used instead of copper anodes in order to prevent the deposition of seed material onto the electrode surface. Moreover, an attempt was made to reduce the impurity contamination by increasing the bottom temperature of the heat exchanger. As a result of these efforts, an output power of 544 kW for thermal input of 3.38 MW and an enthalpy extraction ratio of 18.9% for thermal input of 2.17 MW were successfully demonstrated. Each value is the highest among those achieved with the Fuji-1 facility. In the present paper the results of the recent Fuji-1 experiments are presented in detail.

Fuji-1 Facility and the Disk MHD Generator

A schematic diagram of the Fuji-1 facility is shown in Fig. 1. The explanation of each component was given previously in Ref. 5.

Received 21 May 2002; revision received 22 April 2003; accepted for publication 25 April 2003.

*Professor, Department of Energy Sciences. Member (173745), International.

†Associate Professor, Research Center for Carbon Recycling Energy.

‡Professor Emeritus; currently Professor, Nagasaki University, Nagasaki 852-8521, Japan.

§Professor Emeritus; currently President, Shizuoka Institute of Science and Technology, Shizuoka 437-8555, Japan.

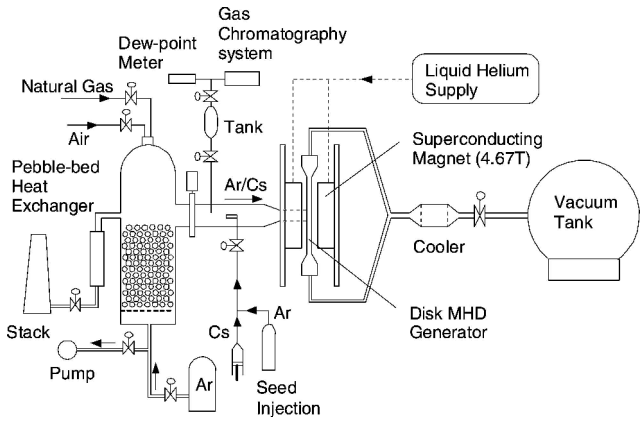

Fig. 1 Schematic diagram of Fuji-1 blowdown facility.

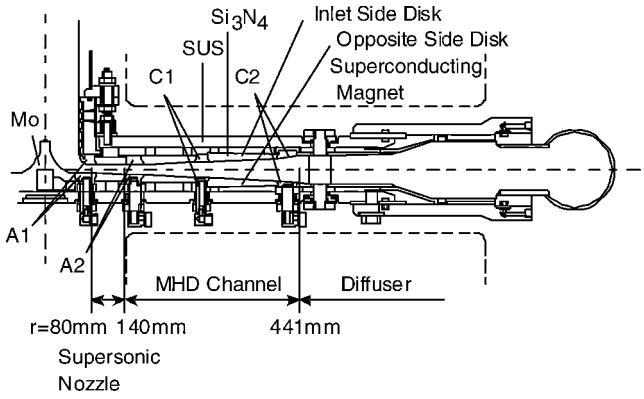

Fig. 2 Cross-sectional view of Disk-F4 generator.

Argon gas is heated to about 2000 K in a pebble-bed-type heat exchanger, and cesium-seed material is mixed with the heated gas in a hot duct through a seed injection nozzle. The cesium-seeded argon working gas is introduced into the disk generator, where the magnetic flux density of about 4.7 T is applied by a Helmholtz-type superconducting magnet. The working gas after passing through the generator is cooled, seed material is recovered in a pebble bed cooler, and introduced into a vacuum tank equipped to achieve a proper pressure ratio between the generator inlet and the exit. It takes about two days for heating up the heat exchanger to the required temperature and about five days for cooling down the superconducting magnet from room temperature to the operating temperature. The time duration of power generation is about 1 min in this system.

The gas temperature and pressure in the hot duct are measured using a platinum–rhodium thermocouple with radiation shield and a pressure transducer, which are regarded as the stagnation temperature and stagnation pressure at the generator inlet, respectively. The seed fraction is estimated from the amount of injected seed material. The impurity measurement system in the present Fuji-1 facility is also illustrated in Fig. 1. A part of the working gas, which passed through the heat exchanger, is extracted from the hot duct and reserved in tanks during the run of power generation. The H_2O concentration in the sample gas is measured by means of a dew-point meter with an accuracy of 10 ppm. Additionally, other impurities such as CO_2, N_2, H_2, and O_2 are detected using a gas chromatography system. Although the seed fraction and impurity concentration strongly influence the generator performance as will be described later, the impurity measurements are not directly taken in the generator channel, but sufficiently upstream of the channel. Therefore, no information of impurity/seed chemistry in nonequilibrium plasma within the MHD generator is available in the present study.

The detailed cross-sectional view of the Disk-F4 generator is shown in Fig. 2. The generator consists of a supersonic nozzle (80 mm $< r <$ 140 mm), MHD channel (140 mm $< r <$ 441 mm), and a diffuser ($r >$ 441 mm). Two ring-typed anodes, first (A1) and second anode (A2), and two cathodes, first (C1) and second cathode (C2), are located on each disk wall. The heights at the throat, MHD channel inlet (upstream edge of A2), and exit (downstream edge of C2) are 15, 17.5, and 45 mm, respectively. The external load resistance is connected between the second anode (A2) and the second cathode (C2). All of the electrodes are made of copper, and the surfaces of A1 and A2 have been coated with 1.5-mm-thick stainless-steel layer in the experiments of run A4126 and A4127. The first cathode (C1) does not function as an electrode in the present generator, but contributes to sustaining the Si_3N_4 insulator walls with high mechanical strength. Electric probes, static-pressure taps, and optical windows are equipped for measurements. The generator output voltage is measured as a potential difference between A2 and C2. The electric probes, made of tungsten wires, are inserted along the radial direction of the channel in order to measure the radial potential distribution. The output voltage and potential distributions are detected through high voltage dividers, isolation amplifiers, and an optical data-transfer system. The output current flowing through the load resistance is measured using a current transformer. Multichannel pressure measurement system with piezoresistive pressure transducers is used to determine the static-pressure distribution. Optical windows are mounted at two locations in the channel to obtain information regarding the cesium line intensity (672.3 nm). All of the electric signals are recorded with analog data recorders and computers through A/D converters.

Experimental Results and Discussion

Before discussing the results of our recent power-generation experiment with Disk-F4 generator, a summary of past experiments with the Disk-F3a and F3r generators is presented briefly. The cross-sectional views of the disk generators for Disk-F3a, F3r, and F4 are compared in Fig. 3, and the typical output power and enthalpy extraction ratio achieved with each generator are plotted in Fig. 4. The typical working conditions and results with the Disk-F3a and F3r generators are listed in Table 1. An enthalpy extraction ratio of 15.7% for thermal input of 2.57 MW (run 6208) and an output power of 517 kW for thermal input of 3.40 MW (run 6209) were obtained with the Disk-F3a generator in 1989 (Ref. 8). The results of Disk-F3a experiment suggested that an increase in the ratio of generator exit area A_{exit} to the inlet area A_{inlet} should provide a higher enthalpy extraction ratio because low static pressure can be maintained in the generator. Based on this finding, a more divergent Disk-F3r generator was designed, where the area ratio A_{exit}/A_{inlet} was increased up to 6.9 from 4.1 used for Disk-F3a. With the Disk-F3r generator, an enthalpy extraction ratio of 18.0% and the corresponding output power of 297 kW were achieved in

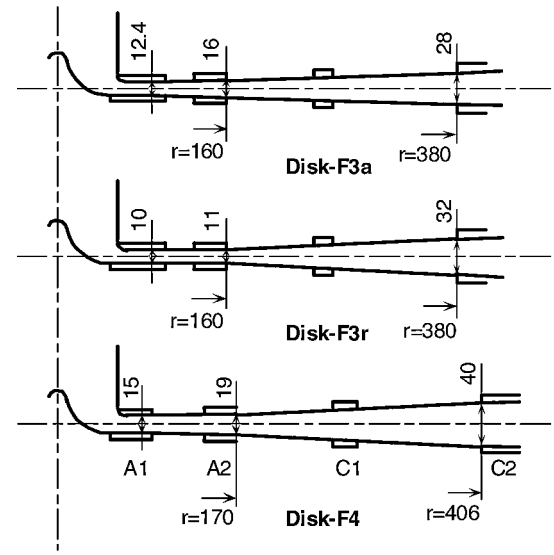

Fig. 3 Disk generators installed in the Fuji-1 facility (Disk-F3a, F3r, and F4). Unit for numerals: millimeters.

Table 1 Typical experimental conditions and results with Disk-F3a and F3r generators

Generator run number	Disk-F3a 6208	Disk-F3a 6209	Disk-F3r A8108
Stagnation pressure, MPa	0.46	0.60	0.24
Stagnation temperature, K	1850	1850	1930
Thermal input, MW[a]	2.57	3.40	1.65
Seed fraction, $\times 10^{-4}$	2.0	1.8	3.0
Load resistance, Ω	0.62	0.49	0.51
A1 and A2 material	Copper	Copper	Copper
Water concentration, ppm	——	Not measured	——
Maximum power output, kW	404	517	297
Maximum enthalpy extraction, %	15.7	15.2	18.0

[a]Thermal input evaluated with the temperature difference from the room temperature of 300 K.

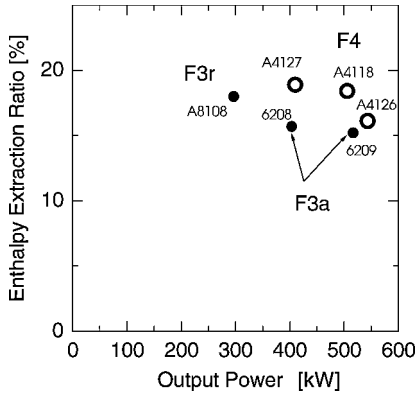

Fig. 4 Output power and enthalpy extraction ratio obtained with Disk-F3a, F3r, and F4 generators.

1992 (Ref. 9). As had been expected, the larger area ratio yielded higher enthalpy extraction ratio. The maximum enthalpy extraction ratio for the Disk-F3r generator was obtained for higher seed fraction of 3.0×10^{-4} as compared to 2.0×10^{-4} used for Disk-F3a. Thus, in a generator with a large area ratio such as the Disk-F3r generator a high enthalpy extraction ratio can be achieved under a high MHD interaction, which is attributed to a high seed fraction.

However, the reproducibility of high power generation with the Disk-F3r was not consistent. The results indicated that from the view point of high power-generation reliability the Disk-F3a generator is better than the Disk-F3r generator. One of the reasons could be that steady nonequilibrium plasma with a high electrical conductivity could not be consistently realized owing to relatively low Mach number at the generator inlet (~2.4). Therefore, as mentioned before, the design goal of the Disk-F4 generator was to achieve better reliability for high power generation. For this purpose the Mach number at the generator inlet was increased to ~2.8. As shown in Fig. 3, the shape of the Disk-F4 generator is nearly similar to that of the Disk-F3a generator, which provided the good reproducibility of power generation. The high Mach number is expected to contribute to the production of nonequilibrium plasma with a high electrical conductivity at the inlet. There is a limitation on the maximum channel height at the generator exit because of the availability of space between the two vacuum vessels of the superconducting magnet in the present Fuji-1 facility. This space limitation forced the height of the channel inlet of the Disk-F3r generator to be small to meet the requirement of a large area ratio A_{exit}/A_{inlet} for a high enthalpy extraction. That limitation led to the results just discussed. On the contrary, because the height at the inlet of Disk-F4 generator is enlarged the area ratio is decreased to 5.0 to meet the same limitation. As it is indicated by the results of the Disk-F3r experiment, one would expect that high enthalpy extraction ratio might not be achieved with the Disk-F4 generator as compared to that achieved with the Disk-F3r generator, because of its small area ratio. However, the generation of plasma with high electron temperature at the generator inlet of the Disk-F4 generator helped to increase the reproducibility of generator power output.

Table 2 Typical experimental conditions and results with Disk-F4 generator

Run number	A4118	A4126	A4127
Stagnation pressure, MPa	0.434	0.545	0.351
Stagnation temperature, K	1980	1973	1914
Thermal input, MW[a]	2.75	3.38	2.17
Seed fraction, $\times 10^{-4}$	2.9	3.7	3.3
Load resistance, Ω	0.48	0.48	0.48
A1-A2 connection, Ω	0 (short)	11	11
A1 and A2 material	Copper	Stainless steel coated	Stainless steel coated
Water concentration, ppm	300	160	160
Maximum power output, kW	506	544	410
Maximum enthalpy extraction, %	18.4	16.1	18.9

[a]Thermal input evaluated with the temperature difference from the room temperature of 300 K.

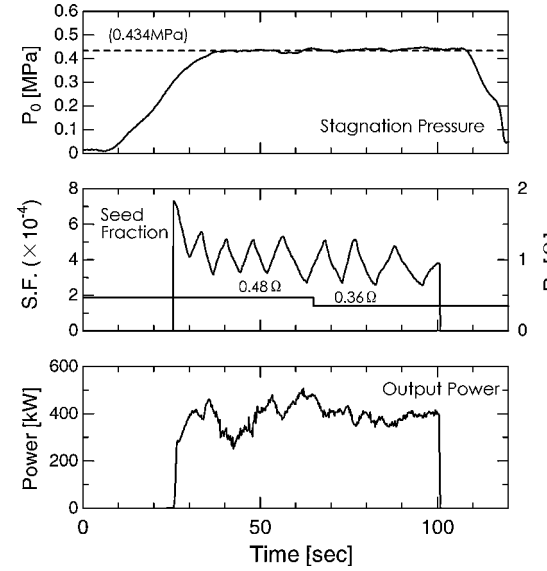

Fig. 5 Time variations of working conditions and output power (run A4118, copper anodes).

Typical working conditions and results with the Disk-F4 generator are listed in Table 2. In the experiment of Run A4118, an enthalpy extraction ratio of 18.4% for thermal input of 2.75 MW was achieved with a large output power of 506 kW. In the last experiments an output power of 544 kW for thermal input of 3.38 MW (run A4126) and an enthalpy extraction ratio of 18.9% for thermal input of 2.17 MW (run A4127) were successfully demonstrated. Each value is the highest among those achieved with the Fuji-1 facility.

Details from the results of run A4118, where both high enthalpy extraction ratio and large output power were achieved simultaneously, are presented in order to clarify the problem revealed in this experiment and the purpose of the last experiment. The time sequence of this experiment is shown in Fig. 5, where the time variations of the stagnation pressure P_0, the load resistance R_L, the seed fraction (S.F.), and the output power (Power) are plotted. Here, the time of 0 s refers to the start of the main phase of blowdown experiment. The parenthesized value of stagnation pressure denotes the time-averaged value during the period, when the stagnation pressure is kept almost constant to the value set for the experiment. In this experiment the seed fraction was continuously changed in the range of 2.6×10^{-4} to 5.2×10^{-4} for two different values of load resistance. As shown in the time variation of output power, the maximum power output of 506 kW was obtained at 62 s under the conditions of the load resistance of 0.48 Ω and seed fraction of 2.9×10^{-4}. The corresponding enthalpy extraction ratio was 18.4%. It can be emphasized here that both high enthalpy extraction ratio and large output power were obtained simultaneously with the Disk-F4 generator.

It is seen from Fig. 5 that the output power diminishes during the period of 40 to 50 s, regardless of the control in seed fraction. This phenomenon was also observed in the other past experiments with the exception of the power-generation runs where the seed injection was delayed on purpose. Thus, the time when the output power diminishes (around Time = 45 s) can be determined not by the time from the start of seed injection (Time = 26 s) but by the time from the start of run (Time = 0 s). This observed behavior implies that seed material might be deposited on the walls of the generator (water-cooled copper electrodes and insulator walls) because the wall temperature could not reach a high value at the early stage of the blowdown experiment. Thus, it can be reasoned that the reduction of the output power during 40–50 s might be attributed to possible wall leakage current and/or effectively low seed fraction caused by the seed deposition. On the contrary, the recovery of the output power after 50 s might be caused by a reduction in leakage current and/or effectively high seed fraction as a result of the seed detachment. Based on the intensity of cesium line measured in the upstream and downstream regions of the generator, the seed deposition could take place rather locally in the upstream region of the generator channel including the supersonic nozzle region. On the basis of the experimental results just mentioned, in the most recent experiment the copper anodes were replaced by those coated with stainless steel, which has low thermal conductivity. This is expected to help in achieving a higher anode surface temperature and in turn would help in preventing deposition of seed material.

Figures 6 and 7 show the time variations of working conditions and output power for run A4126 and A4127, where the generator with stainless-steel-coated anodes was used. In run A4126 the stagnation pressure at the generator inlet was increased to 0.545 MPa (thermal input 3.38 MW), and the seed fraction was continuously changed in the range of 1.4×10^{-4} to 4.1×10^{-4} for four different values of load resistance. The maximum power of 544 kW was obtained at 42 s for a load resistance of 0.48 Ω and a seed fraction of 3.7×10^{-4}. This output power is the highest among those achieved in the Fuji-1 facility. The corresponding enthalpy extraction ratio was 16.1%. In run A4127, on the other hand, the stagnation pressure was decreased to 0.351 MPa (thermal input 2.17 MW). The seed fraction was continuously changed in the range of 2.2×10^{-4} to 6.4×10^{-4}. The maximum power of 410 kW was obtained at 56 s for a load resistance of 0.48 Ω and a seed fraction of 3.3×10^{-4}. The corresponding enthalpy extraction ratio was 18.9%. Thus, the highest enthalpy extraction ratio among those demonstrated with the Fuji-1 facility was recorded.

In comparison with the results of run A4118 shown in Fig. 5, the sudden drop in output power observed at the early stage of the power-generation run is eliminated. Thus, the output power in runs A4126 and A4127 clearly depends on the seed fraction. In a strict sense, the output power seems to be sluggish around 44 s in run A4126 and around 48 s in run A4127.

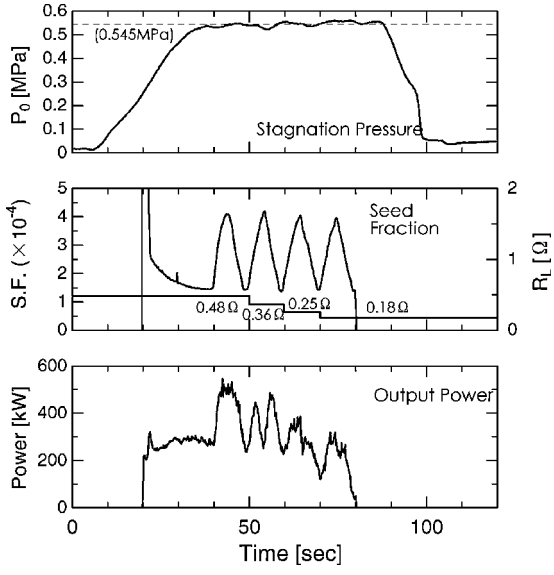

Fig. 6 Time variations of working conditions and output power (run A4126, stainless steel (SUS) anodes).

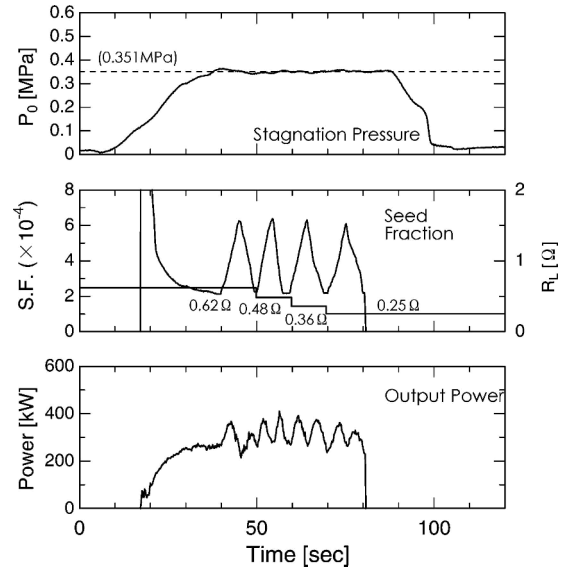

Fig. 7 Time variations of working conditions and output power (run A4127, SUS anodes).

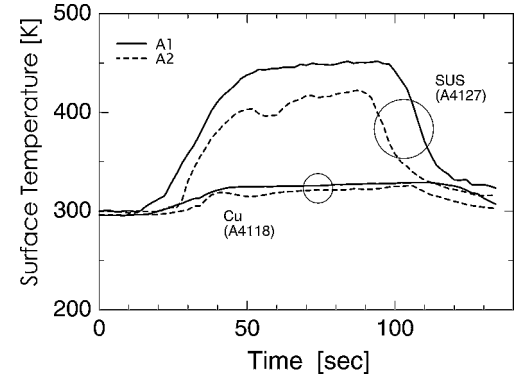

Fig. 8 Time variation of temperature on anode surface.

The temperature on the electrode surface is estimated from the temperature rise in the cooling water. Here the temperature rise refers to the cooling water temperature difference between inlet and outlet of the generator. Figure 8 shows the time variation of the temperature on the surface of first anode (A1) and second anode (A2). It can be noted from this figure that the surface temperature of stainless-steel-coated electrode is higher than that of copper electrode. This is ascribed to the fact that the thermal conductivity of stainless steel is lower than that of copper and that the heat flux to the stainless-steel electrode was lower than that to copper electrode. Under almost the same stagnation pressure and temperature conditions the heat flux to A1 stainless-steel electrode was 1.4–1.5 MW/m^2, whereas the heat flux to A1 copper electrode was 1.7–1.8 MW/m^2. Although many questions still remain unanswered, such as, how accurate is the estimated surface temperature, whether the temperature is high enough to prevent the seed deposition or not, how the increased surface temperature influences the behavior of condensed seed material on the subsequent insulator wall, etc. However, in fact, it was confirmed that the temperature on the surface is increased by using a stainless-steel-coated electrode. This change in electrode material was expected to reduce the deposition of seed material on the electrode (and insulator wall), which in turn resulted in avoiding the sudden drop in output power at the early stage of power generation run, as just mentioned. Therefore, it is verified that the change in material of anode surface is useful to improving the performance of the generator installed in the blowdown facility.

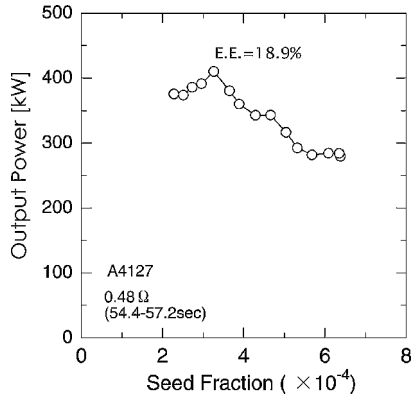

Fig. 9 Output power against seed fraction (run A4127).

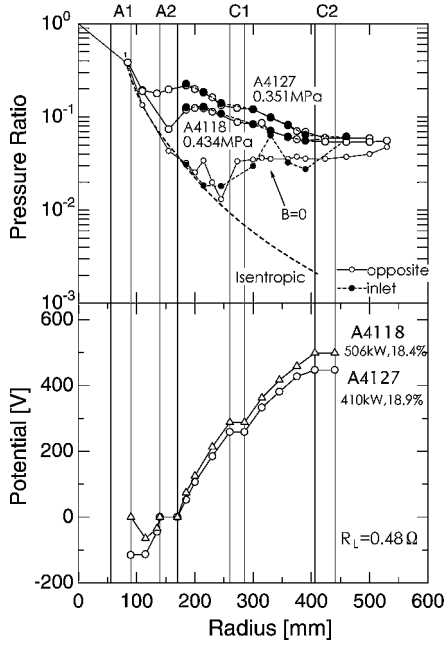

Fig. 10 Radial profiles of electric potential and static pressure. "Opposite" and "inlet" denote the pressure profiles measured on the two disk walls (see Fig. 2.)

The experimental results of run A4127, where the highest enthalpy extraction ratio of 18.9% was achieved, are discussed in detail. As is shown in Fig. 7, the output power clearly responds to the seed fraction for each load resistance. Thus, the output power has two crests for one peak in the seed fraction. This fact indicates that there exists some optimal seed fraction to attain the maximum output power. Figure 9 shows the variation of output power with the seed fraction for a load resistance of 0.48 Ω. For the seed fraction higher than the optimal value, the working gas is thought to be decelerated by the strong Lorentz force. For low seed fraction, on the other hand, the effective electrical conductivity is expected to be low.

Figure 10 shows electric potential and static-pressure profiles in the radial direction of the generator for run A4127, during the maximum output-power condition. In this figure the radial distributions of electric potential and static pressure for run A4118 and the radial distributions of static pressure for run without applying any magnetic field ($B = 0$) are shown for comparison. Here, the static pressures are normalized by the generator inlet stagnation pressures at that moment. Load resistance is connected between the second anode (A2) and the second cathode (C2). The radial static-pressure distribution for $B = 0$ indicates that in the downstream region, starting from C1, the pressure values start deviating from the pressure obtained by isentropic relation, which is caused by flow deceleration and hence the pressure rise in the diffuser region ($r > 441$ mm). Under the condition of the maximum power output, the gradients of the potential, that is, the electric fields, seem to be roughly constant along the generator channel. Also, the electric field in the inlet region of the generator is found to reach about $-4 \sim -5$ kV/m for both the power-generation runs. The static pressure at A2 is higher than that measured for $B = 0$ and compared using the isentropic relation. The pressure increase at A2 can be attributed to the Lorentz force in the supersonic nozzle. It is found here that the pressure at A2 for run A4127 is increased markedly as compared to that for run A4118. This fact is attributed to the relatively low stagnation pressure for run A4127, where there occurred a more effective interaction between plasma and fluid. For run A4118 the pressure increased abruptly in the generator inlet owing to the strong MHD interaction and decreased gradually toward the downstream region. For run A4127, on the other hand, the static pressure decreased with a relatively large gradient because of the high pressure at A2. This fact is expected to be one of the reasons which resulted in the highest enthalpy extraction ratio for run A4127.

As mentioned earlier, one of the main objectives in the Fuji-1 experiments was to demonstrate the high enthalpy extraction ratio, and this goal was successfully achieved in the power-generation experiment with the Disk-F4 generator. To realize the high plant efficiency of a MHD power-generation system, a high isentropic (turbine) efficiency is required. Measurement of stagnation pressure at the generator exit and in the diffuser region was attempted in order to estimate the isentropic efficiency of the present generator. It was found that the measured stagnation pressure was strongly nonuniform along the height direction of the generator. In other words, the flow of working gas has a tendency to move towards either of the disk end walls in the diffuser region. Thus, the isentropic efficiency estimated from the measured stagnation pressure would be unreliable. The isentropic efficiency can be estimated in an alternative way from the enthalpy extraction ratio obtained and the area ratio of generator exit to the throat.[13] Using this approach, the isentropic efficiency of the generator can be evaluated as about 24% for enthalpy extraction ratio of 18.9% for run 4127. This low isentropic efficiency is attributed to the large area ratio of the generator. As has been verified in earlier shock-tube experiments, the large area ratio of the generator yields a high enthalpy extraction ratio and a low isentropic efficiency.[13]

The influence of H_2O vapor contamination in the working gas on the performance of the disk MHD generator installed in the Fuji-1 blowdown facility has been investigated. In the Fuji-1 facility, as just mentioned, argon gas is heated to about 2000 K in a pebble-bed-type heat exchanger. The pebble bed is heated by utilizing the thermal energy of combustion of natural gas. The temperature at the top of the bed reaches 2300 K, whereas the bottom temperature is kept below 850 K, a constraint specified by the mechanical strength of metal grid sustaining the bed. To avoid the contamination of impurities such as H_2O, CO_2, N_2, H_2, and O_2 in the argon gas, the combustion gas is exhausted by vacuum pumps before the start of blowdown during the power-generation experiments. In the experiments, however, a considerable amount of impurities has been detected. In many studies regarding the influence of impurities on the generator performance, it was pointed out that the impurities should result in unsteady and nonuniform plasma and deteriorate the generator performance, where H_2O is considered to be most influential.[14] In the recent power-generation experiments with the Fuji-1 facility, the reliability of impurity concentration measurements has been improved, and consistent results have been obtained.

The maximum enthalpy extraction ratios achieved in several power-generation runs, including the last experiment, are plotted against H_2O concentration in Fig. 11. Because the operating conditions in the experiments such as the stagnation pressure P_0 and temperature T_{g0} at the generator inlet were not the same, it is very difficult to draw any conclusions on the effect of impurity on the enthalpy extraction ratio. However, the enthalpy extraction ratio seems to increase with the reduction of H_2O concentration. Figure 12 shows the potential profile in the radial direction of the generator when the maximum enthalpy extraction ratio was obtained in each experiment. The electric field at the generator inlet for high H_2O concentration is low as compared to that for low H_2O concentration.

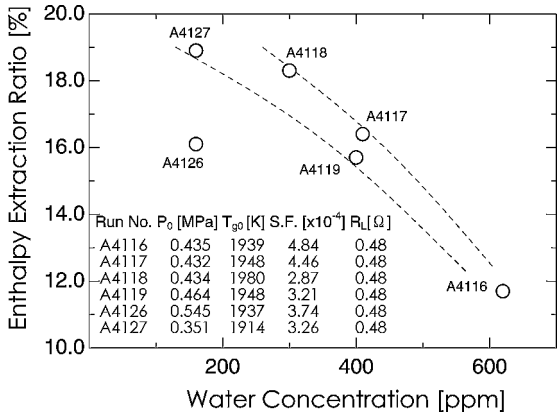

Fig. 11 Enthalpy extraction ratio against H_2O concentration.

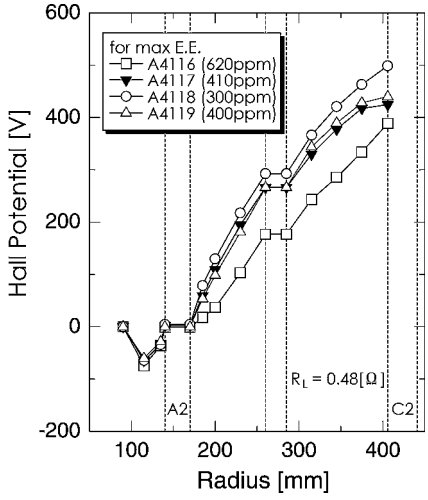

Fig. 12 Potential profile for maximum enthalpy extraction ratio.

Thus, the reduction of output power for high H_2O concentration is attributed to the lower effective electrical conductivity in the inlet region of the generator. At the same time the fluctuation of output power was extremely large for high H_2O concentration. In the power-generation runs of run 4116–4119, where the operating conditions are nearly identical, except some difference in seed fraction, the seed fraction that leads to the maximum enthalpy extraction ratio is decreased with the decrease in the H_2O concentration. This fact indicates that the high electron temperature, that is, nonequilibrium plasma state, can be more easily maintained for low H_2O concentration, which leads to high electrical conductivity even for low seed fraction. In the practical situation the water/seed chemistry would take place in the generator, which should influence the generator performance. However, it is very difficult in the present system to clarify the influence of the water/seed chemistry precisely.

To improve the generator performance, the H_2O concentration needs to be reduced. From the recent experimental results one can notice interesting trends. Figure 13 shows the H_2O concentration as a function of the temperature at the bottom of the pebble bed in the heat exchanger. From this figure the H_2O concentration seems to decrease with the increase in the bottom temperature as indicated by closed-circle data points (past experiments). High H_2O concentrations were also detected regardless of the bottom temperature, as shown by crosses. This could be attributed to the leakage of the combustion gas to the argon supply tube and the hot duct connected to the heat exchanger. Thus, the H_2O concentration is expected to decrease with the increase in the bottom temperature of heat exchanger under careful heat-up operation. The upper limit in the temperature, unfortunately, is restricted by the mechanical strength of metal grid sustaining the pebble bed. The strategy for the reduction of impurity contamination, however, was pointed out. The results in the last experiments are also plotted with open circles. The relation between

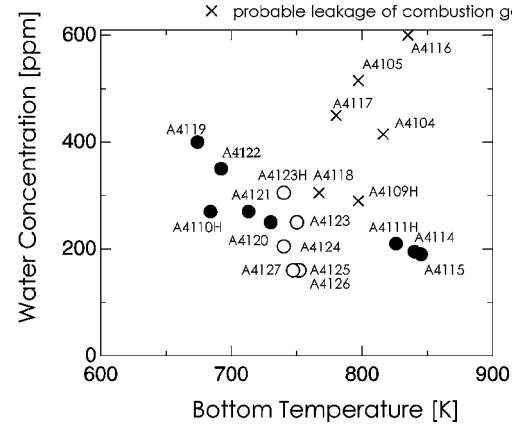

Fig. 13 H_2O concentration as a function of bottom temperature in heat exchanger.

H_2O concentration and the bottom temperature is reconfirmed more concretely.

Finally, a brief comment on the numerical study of the generator performance in the Fuji-1 facility is given. As has been mentioned earlier, the nonequilibrium plasma and fluid behavior in the generator of Fuji-1 facility are very complicated. That is, nonequilibrium seeded plasma with impurity contamination and the fluid flow with shock wave and boundary-layer separation should be simultaneously simulated three dimensionally. Fluid behavior with boundary layer and the impurity effect have been investigated individually with two-dimensional simulation for a disk generator,[15,16] and a three-dimensional simulation for ideal operating conditions has been carried out previously.[17] The complete three-dimensional simulation, including these effects for the Fuji-1 experiment, will be carried out in the near future.

Conclusions

Recent results of the Fuji-1 power-generation experiments are reported herein. In the power-generation experiment with Disk-F4 generator, an output power of 544 kW for thermal input of 3.38 MW and an enthalpy extraction ratio of 18.9% for thermal input of 2.17 MW were successfully demonstrated. Each value is the highest among those achieved in the Fuji-1 experiments.

The sudden drop in output power observed at the early stage of the power-generation run, which could be attributed to the deposition of seed material on the water-cooled anodes and insulator walls, was eliminated in subsequent tests by using the stainless-steel-coated anodes.

It was confirmed that the reduction of impurity contamination resulted in the improvement in the generator performance. To improve further the generator performance, the water vapor concentration needs to be reduced. The reduction can be realized by increasing the bottom temperature of heat exchanger under its careful heat-up operation in the present Fuji-1 system.

Acknowledgments

The authors wish to express great thanks to K. Yoshikawa, K. Ohgaki (Tokyo Institute of Technology), and Y. Hasegawa (National Institute of Advanced Industrial Science and Technology, Japan) for valuable advice and discussion.

References

[1]Rosa, R. J., *Magnetohydrodynamic Energy Conversion*, McGraw–Hill, New York, 1968.

[2]Mitchner, M., and Kruger, C. H., *Partially Ionized Gases*, Wiley, New York, 1973, Chap. 4.

[3]Rosa, R. J., Kruger, C. H., and Shioda, S., "Plasmas in MHD Power Generation," *IEEE Transactions of Plasma Science*, Vol. 19, No. 6, 1991, pp. 1180–1190.

[4]Balemans, W. J. M., and Rietjens, L. H. Th., "High Enthalpy Extraction Experiments with the Eindhoven Blow-Down Facility," *Proceedings of the 9th International Conference on Magnetohydrodynamic Electrical Power Generation*, edited by N. Kayukawa, Vol. 2, Tsukuba, Japan, 1986, pp. 330–340.

[5]Okamura, T., Harada, N., Kabashima, S., Yoshikawa, K., Suekane, T., Tsuji, K., Okuno, Y., Shioda, S., Yamasaki, H., Hasegawa, Y., Matsutani, K., Ishimura, M., Dozono, Y., and Ikeda, S., "Review and New Results of High Enthalpy Extraction Experiments at Tokyo Institute of Technology," *Proceedings of the 32nd Symposium on Engineering Aspects of Magnetohydrodynamics*, 1994.

[6]Nakamura, T., and Riedmuller, W., "Stability of Nonequilibrium MHD Plasma in the Regime of Fully Ionized Seed," *AIAA Journal*, Vol. 12, No. 5, 1974, pp. 661–668.

[7]Yamasaki, H., and Shioda, S., "MHD Power Generation with Fully Ionized Seed," *Journal of Energy*, Vol. 1, No. 5, 1977, pp. 301–305.

[8]Harada, N., Saito, Y., Yoshikawa, K., Yamasaki, H., Kabashima, S., Tsunoda, K., Shioda, S., Hasegawa, Y., Yokota, T., Ishimura, M., Dozono, Y., and Sasaki, T., "High Enthalpy Extraction Demonstration with Closed Cycle Disk MHD Generators," *Proceedings of the 28th Symposium on Engineering Aspects of Magnetohydrodynamics*, 1990, pp. IX3.1–IX3.8.

[9]Harada, Nob., Suekane, T., Okamura, T., Yoshikawa, K., Kabashima, S., Yamasaki, H., and Shioda, S., "Improvement of Generator Performance in FUJI-1 CCMHD Blow-Down Experiment," *Proceedings of the 31st Symposium on Engineering Aspects of Magnetohydrodynamics*, 1993, pp. IVa1.1–IVa1.9.

[10]Okuno, Y., Okamura, T., Yoshikawa, K., Suekane, T., Tsuji, K., Ohgaki, K., Kabashima, S., Shioda, S., Yamasaki, H., Hasegawa, Y., Matsutani, K., Tezuka, M., Ikeda, S., and Mukai, H., "Closed Cycle MHD Power Generation Experiments with FUJI-1 Blow-Down Facility," *Proceedings of the 12th International Conference on Magnetohydrodynamic Electrical Power Generation*, edited by M. Ishikawa, Vol. 1, Yokohama, Japan, 1996, pp. 155–164.

[11]Okuno, Y., Okamura, T., Yoshikawa, K., Suekane, T., Tsuji, K., Okubo, M., Yamasaki, H., Kabashima, S., Shioda, S., and Hasegawa, Y., "High Enthalpy Extraction Experiments with CCMHD Fuji-1 Blow-Down Facility," AIAA Paper 98-2921, June 1998.

[12]Okuno, Y., Okamura, T., Yoshikawa, K., Suekane, T., Tsuji, K., Okubo, M., Yamasaki, H., Kabashima, S., Shioda, S., and Hasegawa, Y., "Power Generation Experiments with CCMHD Fuji-1 Blow-Down Facility," AIAA Paper 99-3659, June 1999.

[13]Yamasaki, H., Okuno, Y., Torii, S., Masuda, J., Tsutsumi, M., Oda, N., Uchiyama, K., Kouka, H., Fujimoto, T., Suzuki, H., Suzuki, M., and Ohgaki, K., "Achievement of Highest Performance in Disk MHD Generator with Ar/Cs," *Proceedings of the International Conference on MHD Power Generation and High Temperature Technologies*, edited by J. Zixiang, Vol. 1, 1999, pp. 233–241.

[14]Dellinger, T. C., and Gray, E. L., "Kinetic Model for Molecular Contamination Effects in Closed Cycle, Nonequilibrium MHD Generators," *Proceedings of the 17th Symposium on Engineering Aspects of Magnetohydrodynamics*, 1978, pp. H.1.1–H.1.9.

[15]Suekane, T., Yoshikawa, K., and Kabashima, S., "The Effects of Boundary Layer Phenomena on the Performance of Disk CCMHD Generator," *IEEE Transactions of Plasma Science*, Vol. 23, No. 1, 1995, pp. 97–102.

[16]Murakami, T., Sasaki, K., Kobayashi, H., Okuno, Y., and Kabashima, S., "Two-Dimensional Simulation of Plasma Structure and Performance of Disk Generator," *Proceedings of the 12th International Conference on Magnetohydrodynamic Electrical Power Generation*, edited by M. Ishikawa, Vol. 2, 1996, pp. 943–952.

[17]Kobayashi, H., Okuno, Y., and Kabashima, S., "Three-Dimensional Structure of MHD Flow in a Disk Generator," *IEEE Transactions of Plasma Science*, Vol. 26, No. 5, 1998, pp. 1526–5131.